ISSN: 2414-1895 DOI: 10.6919/ICJE.202505_11(5).0017

Microstrip Patch Filtering Antenna with High Roll-off Rat

Yiyuan Sun, Hao Ding

School of Physics and Optoelectronic Engineering, Guangdong University of Technology
Guangzhou, 510600, China

Abstract

This paper presents a compact filtering microstrip patch antenna with integrated band-rejection functionality. The design incorporates a dual-layer configuration combining a driven radiator and a parasitic superstrate, achieving a vertical profile of 0.08λ. Three strategically positioned grounding vias and a U-shaped aperture integrated into the primary radiator collectively optimize lower-band suppression (>21.7 dB) while improving transition steepness at the lower operational boundary. Concurrently, the superimposed parasitic layer serves dual purposes: enforcing abrupt roll-off characteristics (>21.9 dB suppression) at the upper band edge and enhancing radiative efficiency.Engineered for the n77 spectrum (3.28–3.85 GHz), the prototype demonstrates a fractional bandwidth of 16% with an average realized gain of 8.0 dBi across the operational band. The architecture exhibits superior spectral confinement, delivering over 21.7 dB rejection in the lower stopband and exceeding 21.9 dB suppression in the upper stopband, outperforming conventional designs in adjacent frequency isolation and in-band performance uniformity.

Keywords

Filtering Antenna; High Out-of-band Suppression; Stacked Patch; Shorting Pins; U-shaped Slot.

1. Introduction

The N77 frequency band (3.3 - 3.8GHz), as an important frequency band for 5G communication, shoulders the heavy responsibility of high-speed and large-capacity data transmission. However, this frequency band is facing an increasingly complex electromagnetic environment, amidst the concurrent operation of heterogeneous radio systems, resulting in acute cross-system interference that degrades signal integrity.Traditional antennas find it difficult to effectively suppress out-of-band interference signals in complex environments, leading to issues such as a decline in communication quality and an increase in the error rate of data transmission.

Some co-design methods for filters and antennas have been proposed. One method is to cascade the filtering circuit and the antenna. The port impedance of the separated filter or antenna is no longer 50 ohms. An optimized impedance is selected at the interface between them [1]. At the same time, it is also very common to use multiple resonators for filtering. In this case, the size can be reduced by utilizing the defected ground plane [2, 3]. In addition, it is quite common to design filtering antennas using magnetoelectric dipoles [4], but it brings a relatively high profile.n recent years, the design method of integrating the filtering circuit with the antenna has also become popular. A filtering functionality can be integrated into a directional loop radiator through the introduction of an auxiliary parasitic element [5]. While traditional filtering antennas exhibit superior gain characteristics, this unidirectional design shows minimal out-of-band suppression effectiveness and lacks competitive advantages in amplification parameters

ISSN: 2414-1895 DOI: 10.6919/ICJE.202505_11(5).0017

The filtering antenna, as an innovative antenna technology capable of combining radiation and frequency-selection functionalities, plays a crucial role in addressing communication challenges within the N77 frequency band. By enabling efficient signal transmission while simultaneously eliminating unwanted out-of-band noise, this integrated solution significantly improves the system's resistance to interference and boosts spectrum efficiency.

The research examines a filtering patch antenna configuration demonstrating improved suppression of out-of-band frequencies and consistent gain stability. The design integrates a primary radiating element (driven patch) with an additional layered parasitic element (stacked patch) positioned vertically above it.

The cascaded patch configuration serves dual purposes: extending operational bandwidth while enhancing radiation efficiency, concurrently creating a marked radiation minimum at the upper operational band limit. Within the primary radiating element, strategic implementation of three grounding vias combined with a precisely-engineered U-shaped aperture functions as controlled impedance discontinuities to establish dual null regions within the lower frequency attenuation spectrum.

Meanwhile, microstrip line feeding is adopted, which does not require an additional complex matching network, making the design simpler and the overall structure more compact.

2. Organization of the Antenna Architectur

2.1 Antenna Architecture and Frequency-Selective Radiative Coupling

2.1.1 Antenna Architecture

The structure of the designed filtering antenna is depicted in Fig. 1, comprising dual patch layers integrated with a ground plane. This configuration utilizes a stacked arrangement where radiating elements are vertically aligned, achieving both filtering characteristics and compact spatial organization. The upper and lower metallic patches work cooperatively to control electromagnetic wave propagation, while the ground plane provides impedance matching and radiation pattern optimization.

The structural details presented in Fig.1(c) reveal a multilayer architecture where the driven radiator and ground plane are respectively fabricated on opposing surfaces of the secondary substrate (ε_r=2.2, thickness h=1.524mm, lateral dimensions l×l). This excitation element, with physical dimensions l_2 ×w_2, incorporates three grounding vias and a magnetically-coupled U-aperture to establish dual-band filtering characteristics. A $\lambda/4$ microstrip feedline terminates at the radiator's edge center for optimized impedance matching, while an h_1-height air spacer strategically separates the dielectric substrates. Section III will systematically analyze the electromagnetic coupling mechanisms enabling this configuration's operation.

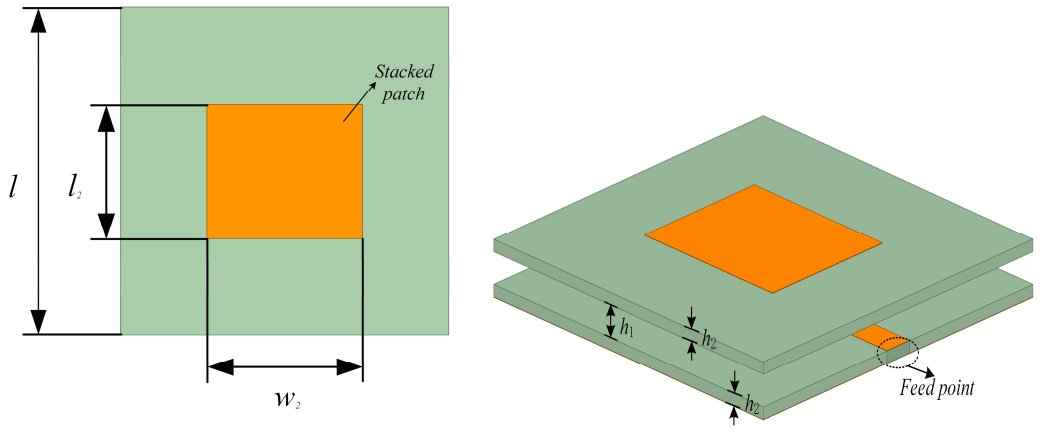

(a) (b)

ISSN: 2414-1895 DOI: 10.6919/ICJE.202505_11(5).0017

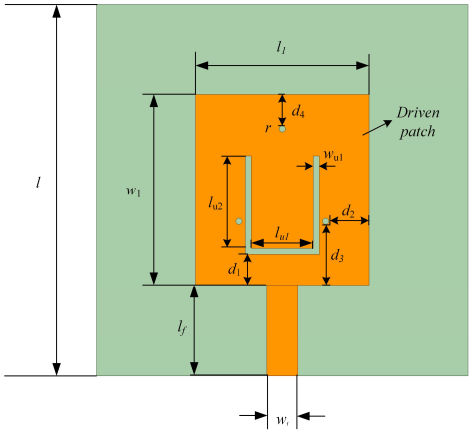

(c)

Fig. 1 (a) Upper stacked patch. (b) Side view of the proposed antenna. (c) Upper Driven patch with a U-slot and three shorting pins.

2.1.2 Frequency-Selective Radiative Coupling

To develop a filtering antenna with optimized operational characteristics, a multi-layer patch structure is employed to enable the realization of extended stopband coverage and improved radiation efficiency, complemented by a microstrip-based feeding mechanism.

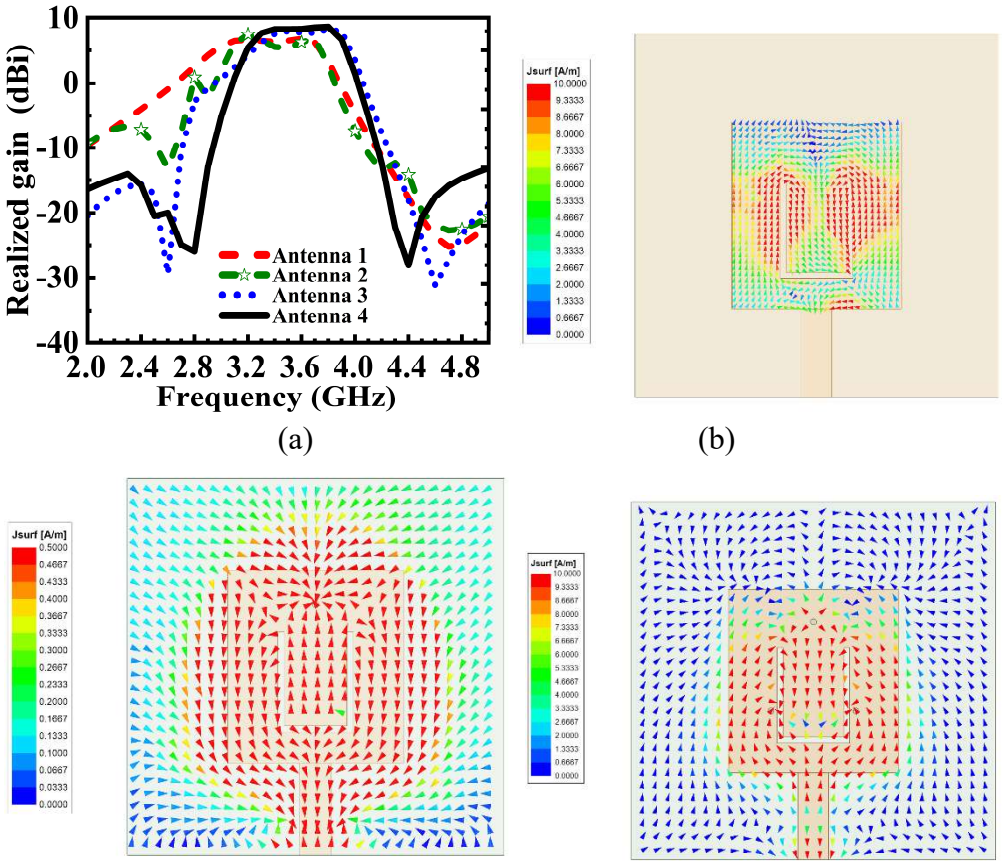

(a) (b)

(c) (d)

Fig. 2 Realized gains for the antenna (a) Measured gain characteristics of four configurations:Ant1: No U-slot/short-circuit paths,Ant2: U-slot implementation Ant3: U-slot + single grounding via,Ant4: U-slot + triple grounding vias..(b) . Surface current distributions at 2.85 GHz (U-slot variant). (c) . Current vector mapping at 3.70 GHz (U-slot + 1 via) (d) . Eddy current manifestations at 2.75 GHz (U-slot + 3 vias)

ISSN: 2414-1895 DOI: 10.6919/ICJE.202505_11(5).0017

By adopting the stacked patch design, it can be found that, as shown in Fig 2 (a) antenna1 (without U-slot and shorting pins), a zero point (3.7 GHz) is introduced at the edge of the high-frequency band. In order to further improve the filtering performance, a U-shaped slot is introduced on the driving patch, as shown in Fig 2 (a) antenna2 (with U-slot). Analysis of the U-shaped slot's current distribution in Fig.2(b) reveals counter-rotating currents with matched intensity along its perimeter. This flow pattern induces a radiation null at 2.85 GHz adjacent to the lower operational frequency range. Nevertheless, unsatisfactory stopband attenuation characteristics are observed, evidenced by suboptimal roll-off steepness and limited null depth enhancement.

The electrical performance is enhanced by incorporating a grounding via proximal to the periphery of the primary radiator. At this time, we can find that, as shown in Fig 2 (a) antenna3 (with U-slot and 1 shorting pin), the zero point in the low-frequency range becomes more obvious. From the current diagram in Fig 2 (c), it is evident that reverse currents are generated centered around the shorting pin. However, the in-band gain is not stable enough, the passband is relatively narrow, and the out-of-band roll-off rate is not large enough.

Based on this principle, three additional shorting pins are incorporated to enhance the out-of-band roll-off characteristics while expanding the operational bandwidth1. The current distribution depicted in Fig 2(d) reveals counter-directional current flows surrounding all three metallic interconnects, effectively introducing a filtering zero point at 2.75 GHz. As evidenced by the radiation pattern analysis in Fig 2(a) (Antenna4 configuration with U-slot and triple-pin structure), the optimized design achieves.

2.2 Parametric Studies

2.2.1 The Influence of the Driven Patch

The size of the patch has a certain influence on the performance of the antenna. Firstly, the influence of the size of the driving patch on the antenna performance was studied. Figs 3(a) and 3(b) show the simulated reflection coefficients and gains under different patch lengths w_1.

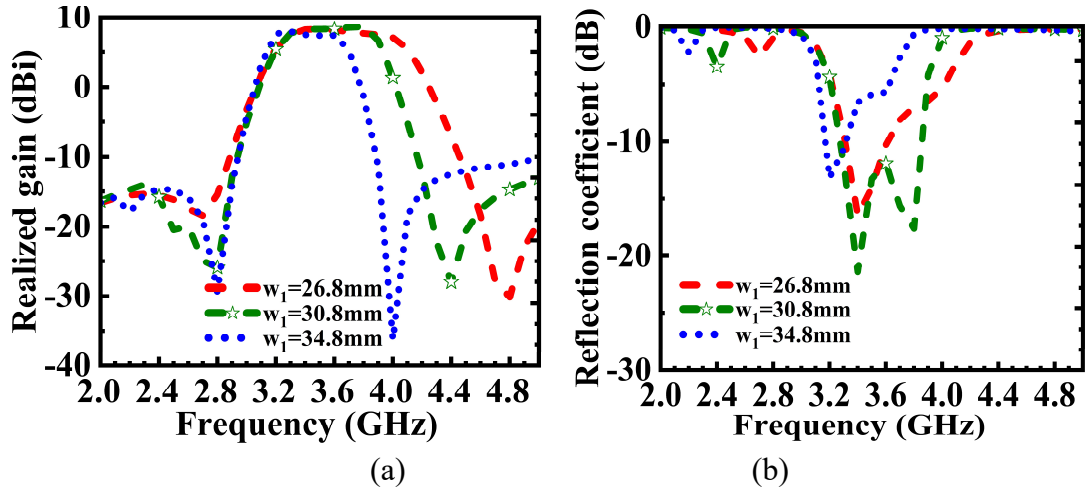

Fig. 3 Influence of Driven Patch Width (W1) on Impedance Characteristics and Radiation Performance (a) realized gain. (b) reflection coefficient

According to the results presented in Figs 3(a) and 3(b), the high-frequency radiation null moves toward lower frequencies with increasing w1 values, while the low-frequency null remains largely unaffected. This phenomenon occurs because the U-shaped slot primarily governs the low-frequency null. The experimental data reveals that 30.8 mm represents the optimal length for parameter w1.

ISSN: 2414-1895 DOI: 10.6919/ICJE.202505_11(5).0017

2.2.2 The Effect of the Interval between the Two Patches

The influence of adjusting the spacing (h1) between the driving patch and the stacked patch is demonstrated in Figures 4(a) and 4(b). As h1 increases from 2 mm to 6 mm, the resonant frequency exhibits minimal variation, while the input impedance undergoes significant alterations. Figure 4(b) reveals that at h1 = 2 mm, the high-frequency band edge displays a sharp roll-off characteristic, though this configuration leads to diminished suppression performance. Conversely, antennas with h1 = 6 mm demonstrate opposite behavior. To achieve a balanced design, the prototype adopts an intermediate spacing of h1 = 4 mm.

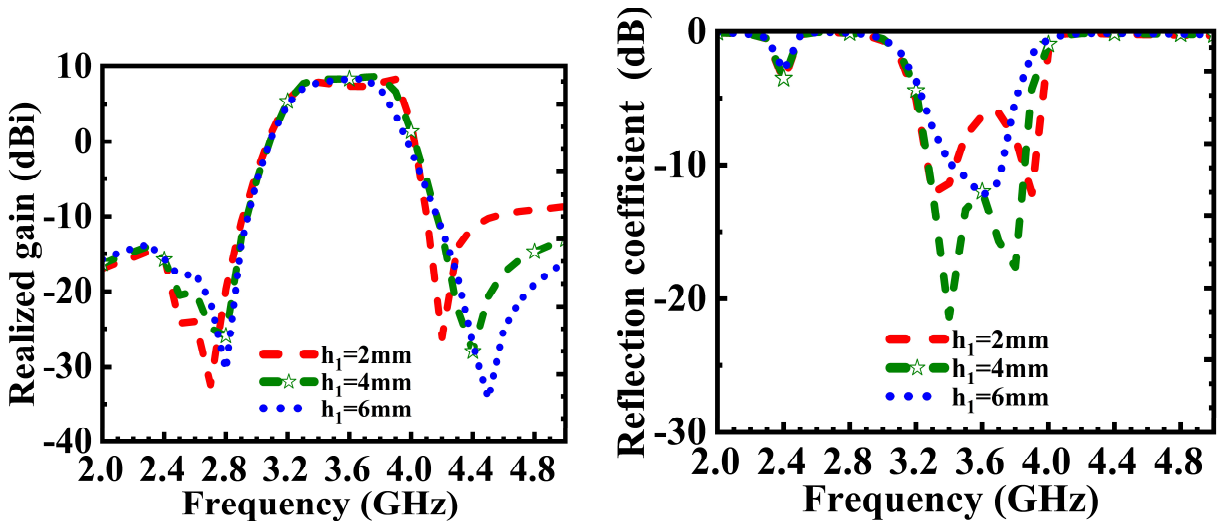

(a) (b)

Fig. 4 The influence of the interval between the two patches on (a) reflection coefficient and (b) realized gain.

The simulated radiation patterns of antenna at 3.28, 3.6, and 3.85 GHz are shown in Fig. 5.

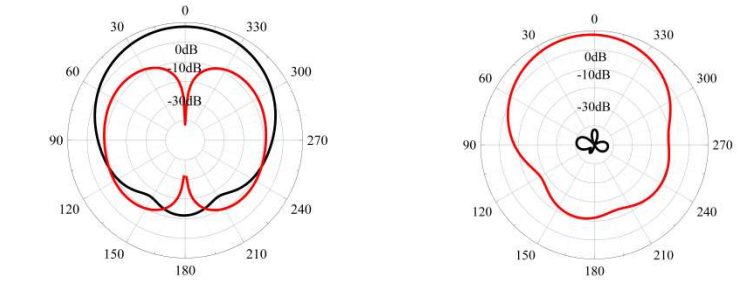

(a)

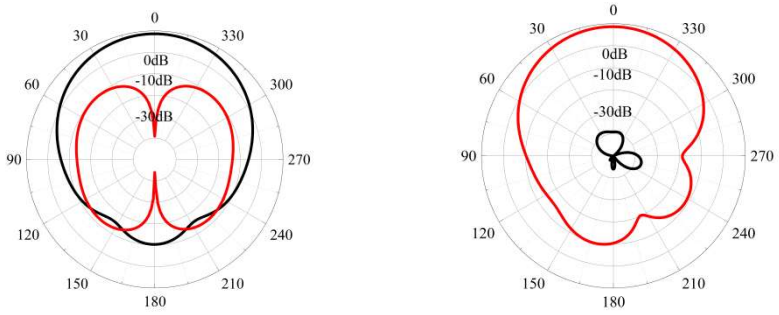

(b)

ISSN: 2414-1895 DOI: 10.6919/ICJE.202505_11(5).0017

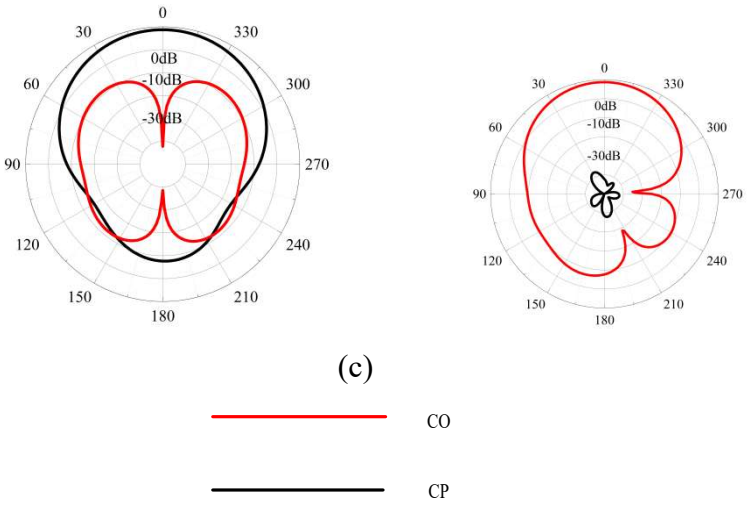

Fig. 5 Simulated and measured radiation patterns of the antenna in E-plane and H-plane at (a) 3.28, (b) 3.60, and (c)3.85 GHz.

3. Summary

This research investigates a high-selectivity filtering patch antenna featuring enhanced out-of-band rejection while maintaining effective radiation characteristics. The operational mechanism is thoroughly analyzed, demonstrating that the integrated design of layered radiating elements, U-slot configurations, and grounding pins enables precise generation and regulation of three radiation nulls beyond the operational band. These structural innovations yield exceptional frequency selectivity with a roll-off rate reaching 39.7 dB/GHz and out-of-band suppression surpassing 21 dB. Characterized by structural simplicity, the proposed antenna simultaneously delivers stable radiation performance with an average gain around 8.0 dBi within the operational bandwidth.

Table 1. Length of the proposed antenna

Parameter	l	h_1	l_1	w_1	lu_1	wu_1	lu_2	r	h_2
Value(mm)	60	4	28	30.8	10	1	16	0.5	1.524
Parameter	l_2	w_2	w_f	l_f	d_1	d_2	d_3	d_4	
Value(mm)	24.5	28.5	5	14.6	5	6.5	9.8	5	

Table 2. Comparison with Existing studies

Numble	Radiators	Gain(dBi)	Rejection level(dB)
[1]	1	4.3	7
[4]	2	8	16.6
[5]	2	4.4	13
This work	2	8	21.7

References

[1] J.-H. Zuo, X.-W. Chen, G.-R. Han, L. Li, and W.-M. Zhang, “An integrated approach to RF antenna-fifilter co-design,” IEEE Antennas Wireless Propag. Lett., vol. 8, pp. 141–144, Apr. 2009.

[2] R. Hou, J. Ren, M. Zuo, X. Du and Y. Z. Yin, "Magnetoelectric Dipole Filtering Antenna Based on CSRR With Third Harmonic Suppression," in IEEE Antennas and Wireless Propagation Letters, vol. 20, no. 7, pp. 1337-1341, July 2021, doi: 10.1109/LAWP.2021.3080037.

ISSN: 2414-1895 DOI: 10.6919/ICJE.202505_11(5).0017

[3] X.-W. Chen, F.-X. Zhao, L.-Y. Yan, and W.-M. Zhang, “A compact fifiltering antenna with flflat gain response within the passband,” IEEE Antennas Wireless Propag. Lett., vol. 12, pp. 857–860, Jul. 2013.

[4] B. Ding, X.-B. Wei, C. Wang, M.-X. Zhang, Z.-T. He, and Y. Shi, “A compact printed fifiltering antenna with flflat gain using annular slot and UIR,” in Proc. 15th Int. Conf. Electron. Packag. Technol., Aug. 2014, pp. 1252–1255.

[5] J.-N. Wu, Z.-Q. Zhao, Z.-P. Nie, and Q.-H. Liu, “A printed unidirectional antenna with improved upper band-edge selectivity using a parasitic loop,” IEEE Trans. Antennas Propag., vol. 63, no. 4, pp. 1832–1837, Jan. 2015.